Optimum Design of Reverse Osmosis Systems for Hydrogen Peroxide Ultrapurification

Ricardo Abejón, Aurora Garea, Angel Irabien
Dept. de Ingeniería Química y Química Inorgánica, Universidad de Cantabria, Santander 39005, Cantabria, Spain

DOI 10.1002/aic.13763
Published online February 15, 2012 in Wiley Online Library (wileyonlinelibrary.com).

This work is focused on the optimization of a reverse osmosis network proposed for the ultrapurification of chemicals, from technical grade to semiconductor grades demanded in electronic applications that require the use of high-purity wet chemicals in the semiconductor manufacturing, as it is the case of hydrogen peroxide that is commonly used in the wafer cleaning and surface conditioning processes. An industrial installation able to produce simultaneously the five different Semiconductor Equipment and Materials International Grades of hydrogen peroxide is represented by a simplified superstructure configuration formulated as a nonlinear programming problem. The network integrates reverse osmosis membrane modules, mixers, and split functions, defined by the equations of mass balances and the Kedem–Katchalsky transport model for the description of the permeate flux and the metal rejection coefficients at each membrane stage. The objective of the design is to maximize the daily profit obtained from the sale of the electronic grades of hydrogen peroxide produced by the ultrapurification system. *AIChE J,* 58: 3718–3730, 2012
Keywords: reverse osmosis, membrane cascades, hydrogen peroxide, ultrapurification

Introduction

Semiconductor manufacturing involves a highly complex and delicate process, and a great variety of high-purity chemicals are required. As a typical silicon wafer might spend the equivalent of 2 days immersed in various liquids (specifically called wet chemicals) during the manufacturing process, the importance of extremely low levels of impurities in these wet chemicals becomes critical.[1] Ionic impurities in the wet chemicals cause problems resulting in the device failures.[2]

Aqueous hydrogen peroxide is among the most commonly used wet chemicals in semiconductor manufacturing.[3] The traditional approach of wafer cleaning and surface conditioning is based on aqueous chemical processes that typically use hydrogen peroxide mixtures.[4] The hydrogen peroxide demand in electronic applications along the last two decades and near-future forecast are depicted in Figure 1.[5] The same graph also shows the percentage of total wet chemicals demand corresponding to hydrogen peroxide. The demand of hydrogen peroxide continues growing despite the static importance of this chemical among the wet chemicals. The likely decrease of relative contribution of hydrogen peroxide is due to alternatives technologies.[6] Environmental health and safety issues are promoting the substitution of the strong chemicals used by this industrial sector, including hydrogen peroxide.[7,8] However, hydrogen peroxide has also found new chances in this green revolution of the semiconductor industry.[9–13]

Correspondence concerning this article should be addressed to R. Abejón at abejonr@unican.es.

Semiconductor Equipment and Materials International (SEMI) is the global industry association serving the manufacturing supply chains for the microelectronic, display, and photovoltaic industries. This association develops the worldwide most respected technical standards in this field. Among all the topics regulated, SEMI Document C30-1110 standardizes requirements for hydrogen peroxide used in the semiconductor industry.[14] The requirements for hydrogen peroxide listed in Table 1 define five different electronic grades (Grades 1–5). Although typically commercialized grades of hydrogen peroxide have been treated by traditional purification techniques (L–L extraction, adsorption, membrane technologies, distillation, etc.) for reducing impurity levels, the very low content of contaminants demanded by the semiconductor industry requires of further ultrapurification treatment.[15] While the least strict electronic grade (Grade 1) can be achieved by expert selection from technical grade and little additional treatment (filtration), the more exigent electronic grades require employment of further ultrapurification technologies.[16]

When the patents published over the last 20 years about ultrapurification of hydrogen peroxide for electronic purposes are reviewed,[17] ion exchange emerges as the most frequently mentioned technology; but distillation is also widely used, especially for organic contamination reduction. Despite the wide number of different adsorbents that have been tested for hydrogen peroxide ultrapurification, this technology has become obsolete because of its low maximum efficiency when compared to other alternative options. All these referenced separation techniques could be replaced by membranes with lower operating expenses due to energy and chemicals.[18] Some patents based on reverse osmosis can be found, but reverse osmosis is still not a dominant

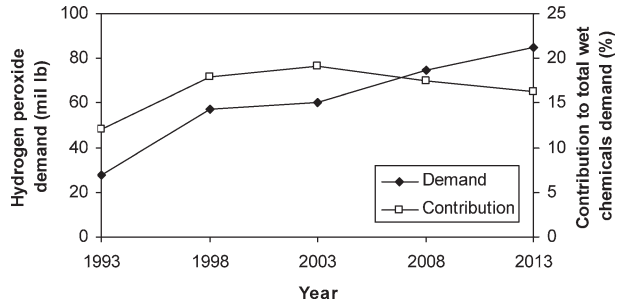

Figure 1. Evolution of hydrogen peroxide demand in electronic applications and contribution to total wet chemicals demand (based on Ref. 5).

ultrapurification technology, as membranes are used in combination with other separation techniques (mainly ion exchange) in hybrid processes. However, this research group has demonstrated recently the technical and economic viability of a reverse osmosis process without auxiliary techniques for production of electronic grade hydrogen peroxide.[17,19]

Reverse osmosis membrane systems are mainly used for seawater and brackish water desalination, as this application has become the main source for supplying fresh water in the regions suffering from scarcity of natural fresh water resources.[20] The typical installation consists of a network of modules designed to fulfill technical, economic, and environmental requirements.[21–24] The complete optimization of a reverse osmosis network has to include the optimal design of both individual modules and the network configuration. The performance of individual reverse osmosis modules in terms of particular module geometry and design and operational conditions has been widely analyzed,[25–30] so suitable transport equations to describe the behavior of membrane modules are available to be applied to module optimization. The optimal configuration of reverse osmosis networks themselves had been less investigated,[31] but recently, several research groups have focused their efforts on the research of optimum design of reverse osmosis systems based on the previous pioneer works.[32–44] The configuration of reverse osmosis networks can be described by the use of stream distribution and matching boxes, designed to represent all possible combinations of stream splitting, mixing, bypass, and recycle.[45] By this formulation, all possible structure arrangements are considered, and the resulting mathematical optimization model can be solved as a mixed integer nonlinear programming (MINLP) problem. However, this network model can be simplified if the splitting boxes are considered as junctions.[46] In this case, the model can be formulated as a NLP problem by consideration of variable split ratios.

Table 1. Requirements for Electronic Grade Hydrogen Peroxide According to SEMI Standard

SEMI Electronic Grade	Assay (H_2O_2, %)	Total Oxidizable Carbon (TOC) Limit (ppm)	Anion Limit Range	Cation Limit Range
1	30–32	20	2–5 ppm	10–1000 ppb
2	30–32	20	200–400 ppb	5–10 ppb
3	30–32	20	200–400 ppb	1 ppb
4	30–32	10	30 ppb	100 ppt
5	30–32	10	30 ppb	10 ppt

This study investigates the optimization of a reverse osmosis network used for ultrapurification of hydrogen peroxide from technical grade to semiconductor grades. An industrial installation able to produce the five different SEMI Grades is represented by a simplified superstructure formulated as a NLP problem. A membrane transport model adequate to describe the permeation of aqueous hydrogen peroxide solutions through reverse osmosis membranes is presented. The model is useful for the optimum selection of design (recovery rates) and operation (applied pressures) conditions and the configuration of the entire network.

Transport Model for Reverse Osmosis

The ion exclusion model has been used to describe the permeation of hydrogen peroxide through reverse osmosis membranes. This model had been previously applied for estimation of the permeation of weakly dissociated compounds in purification and ultrapurification processes by membranes technologies.[47,48]

The derivation of the ion exclusion model is based on the following assumptions (Figure 2):

- All ions are excluded by the membrane (double layer effect).
- All species in molecular form permeate the membrane completely.
- Perfect mixing conditions prevail on the retentate and permeate sides of the membrane.
- Concentration polarization is ignored.

The final equation for estimating the permeate concentration (x_P) from the feed concentration (x_F) is presented as Eq. 1 (the complete derivation of the ion exclusion model equation was published by Kulkarni et al.[48]). The only required parameter in Eq. 1 is the dissociation constant of the molecule to permeate.

$$x_P = x_F - \sqrt{K_A \cdot x_F} - \sqrt{K_A\left(x_F - \sqrt{K_A \cdot x_F}\right)} \qquad (1)$$

For the particular case of hydrogen peroxide, it can be considered as weakly acidic in aqueous solution, having a pK_A

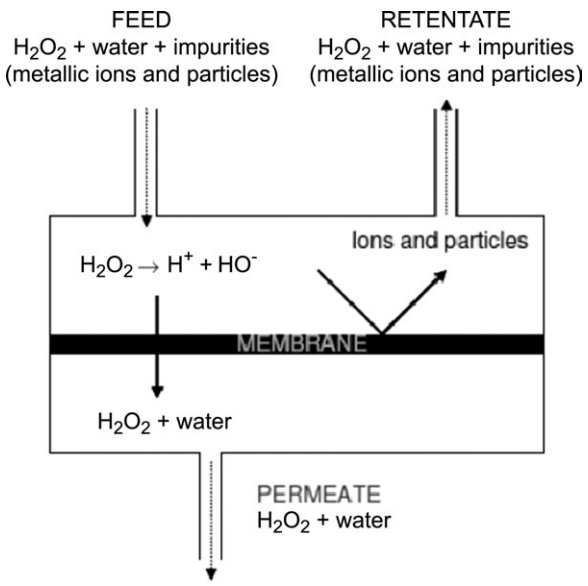

Figure 2. Schematic diagram of mass transfer through a reverse osmosis membrane for hydrogen peroxide aqueous solutions.

Table 2. Kedem–Katchalsky Model Parameters for Reverse Osmosis Membrane in Hydrogen Peroxide Solution Medium

	B	Na	Al	Ti	Cr	Mn	Fe	Ni	Cu	Zn
ω'^{metal} (m/d)	0.482	0.023	0.029	0.044	0.062	0.216	0.121	0.035	0.101	0.132
σ^{metal}	1.000	0.926	0.920	0.917	0.925	1.000	0.928	0.920	1.000	0.964
L_P (m/s bar)	4.92×10^{-7}									

of 11.75 ($K_A = 1.78 \times 10^{-12}$ M) at 20°C.[15] The dissociation of the second proton is insignificant.[49] When the model was applied to feed concentrations limited by the minimum and maximum values of allowed SEMI Standard, namely, 30–32% (equivalent to x_F values in the range 8.8–9.4 M), the resultant permeate concentrations (x_P) predicted by the model reached values upper than 99.999% of their corresponding feed concentrations. These results imply no theoretical dilution of aqueous hydrogen peroxide solutions when forced to permeate through reverse osmosis membranes. Experimental determination of hydrogen peroxide concentration in both feed and permeated streams of a lab-scale reverse osmosis installation confirmed the performance predicted by the ion exclusion model.[17]

Once the validity of reverse osmosis for aqueous hydrogen peroxide solutions without practical dilution or concentration effects was asserted, the technical grade hydrogen peroxide could be considered as a unique solvent matrix (aqueous hydrogen peroxide solution) with several solutes (metallic impurities). Numerous transport models for reverse osmosis membrane separations can be found in bibliographic sources.[50] Some of the most common models were tested for the representation of the performance of the technical grade hydrogen peroxide ultrapurification process by means of a lab-scale experimental installation working with a polyamide flat-sheet reverse osmosis membrane.[17] The Kedem–Katchalsky model was considered the most suitable for representing the performance of the reverse osmosis process, when used in the ultrapurification of aqueous hydrogen peroxide solutions.[51] The Kedem–Katchalsky model has been widely used for predicting the behavior and performance of reverse osmosis systems[52–54] and other membrane separations as nanofliltration and ultrafiltration.[55–57]

The Kedem–Katchalsky model is based on three parameters: the solvent permeability of the membrane (L_P), the coefficient of solute mobility (ω), and the reflection coefficient (σ). According to the model, the solvent and solute fluxes (J_V and J_S respectively) are given as follows

$$J_V = L_P\,(\Delta P - \sigma\Delta\Pi) \tag{2}$$

$$J_S = \omega\Delta\Pi + \,(1-\sigma)\,J_V(C_S)_{ln} \tag{3}$$

where ΔP is the applied pressure, $\Delta\Pi$ is the osmotic pressure difference across the membrane, and $(C_S)_{ln}$ logarithmic average solute concentration across the membrane. For the particular case of ultrapurification applications, the osmotic pressure difference can be neglected ($\Delta\Pi \approx 0$), as confirmed by the agreement between the values of the solvent fluxes for ultrapure water and water doped with metallic ions in the low ppm level.[17] Hence, Eq. 2 can be simplified by elimination of the osmotic pressure term

$$J_V = L_P\,\Delta P \tag{4}$$

showing a proportional relationship between solvent flux and applied pressure (the solvent permeability L_P behaves as proportionality coefficient between both variables). The solute flux J_S is not a practical variable, when tackling the management of reverse osmosis systems and the solute rejection coefficient appears as a more practical variable. The rejection coefficient (R) is defines as

$$R = \frac{C_F - C_P}{C_F} \tag{5}$$

where C_F and C_P represent the solute concentration on the feed and permeate streams, respectively. The rejection coefficient R can be expressed in terms of the Kedem–Katchalsky parameters by Pusch's approach[58,59]

$$R = \frac{\sigma\,J_V}{J_V + \omega'} \tag{6}$$

where ω' is the modified coefficient of solute mobility obtained by application of the Morse equation (Eq. 7) for conversion of the osmotic pressure difference to concentration difference

$$\Pi = \; m\,i\Re T \tag{7}$$

$$\omega' = \; \omega v\Re T \tag{8}$$

where $\Re$ is the gas constant, T the temperature, i the van 't Hoff factor, m the solute molar concentration, and v a stoichiometric coefficient based on van 't Hoff factor.

The equations of the reverse osmosis model have been incorporated to the optimization programming with the corresponding parameters derived from experimental results. The estimation of the Kedem–Katchalsky parameters for hydrogen peroxide ultrapurification by reverse osmosis membrane had been previously carried out by this research group according to experimentally obtained values of permeate flux and rejection coefficients for varying applied pressures.[17] The obtained parameters are listed in Table 2.

Superstructure Configuration

The typical module arrangements for reverse osmosis networks can be categorized as straight-through, tapered, or cascade designs.[31] The straight-through and tapered arrangements are multistage systems with several modules in parallel in each stage. In the straight-through scheme, the number and size of the modules are identical for every stage, whereas in the tapered scheme, the number or the size of the modules decreases over successive stages. Both arrangements can be modified by addition of recycle and bypass streams or inclusion of retentate or permeate reprocessing. On the other hand, cascade design of reverse osmosis systems follows the principles for multistage fractionation columns: multipass permeate configuration is applied to purify the permeate, when the target solute rejection cannot be accomplished in a single stage, and reflux is reproduced by stream recycling for each stage.

As a previous work of this research group,[60] the applicability of reverse osmosis membrane cascade configuration

Table 3. Feeding Conditions (Concentrations of Metals and Flow of the Feed Stream *F*)

Concentration (ppb)	
B	8
Na	25000
Al	1300
Ti	80
Cr	55
Mn	5
Fe	200
Ni	30
Cu	3
Zn	15
Flow (m^3/d)	24.19

to hydrogen peroxide ultrapurification was investigated. The number of stages required for obtaining each electronic grade was determined by means of simulation, based on the cation limit range (Table 3), and the results show viable installations from two to seven stages (corresponding to SEMI Grade 1 and 5, respectively). Based on these results, the superstructure shown in Figure 3 was designed. It represents a seven-stage countercurrent cascade system able to produce simultaneously all the different SEMI Grades. The network integrates reverse osmosis membrane modules, mixers, and split junctions. The complete mathematical model that describes the superstructure was formulated as follows by the appropriate equations based on mass balances and the Kedem–Katchalsky transport model.

Mixers:

$$Q(i)_{\text{mixin1}} + Q(i)_{\text{mixin2}} = Q(i)_{\text{mixout}} \tag{9}$$

$$Q(i)_{\text{mixin1}} C(i)^{\text{metal}}_{\text{mixin1}} + Q(i)_{\text{mixin2}} C(i)^{\text{metal}}_{\text{mixin2}} = Q(i)_{\text{mixout}} C(i)^{\text{metal}}_{\text{mixout}} \tag{10}$$

where $Q(i)_{\text{mixin1}}$, $Q(i)_{\text{mixin2}}$ and $C(i)^{\text{metal}}_{\text{mixin1}}$, $C(i)^{\text{metal}}_{\text{mixin2}}$ denote, respectively, the flows of the streams entering the i mixer and the corresponding concentrations of each metal in the same streams, and $Q(i)_{\text{mixout}}$ and $C(i)^{\text{metal}}_{\text{mixout}}$ denote the flow of the stream leaving the i mixer and the respective metal concentration, respectively.

Split junctions:

$$Q(j)_{\text{splitin}} = Q(j)_{\text{splitout1}} + Q(j)_{\text{splitout2}} \tag{11}$$

$$Q(j)_{\text{splitin}} X(j)_{\text{split}} = Q(j)_{\text{splitout1}} \tag{12}$$

$$C(j)^{\text{metal}}_{\text{splitin}} = C(j)^{\text{metal}}_{\text{splitout1}} = C(j)^{\text{metal}}_{\text{splitout2}} \tag{13}$$

where $Q(j)_{\text{splitin}}$ and $C(j)^{\text{metal}}_{\text{splitin}}$ denote the flow of the stream entering the j split junction and the corresponding concentration of each metal in the same stream and $Q(j)_{\text{splitout1}}$, $Q(j)_{\text{splitout2}}$ and $C(j)^{\text{metal}}_{\text{splitout1}}$, $C(j)^{\text{metal}}_{\text{splitout2}}$ denote the flows of the streams leaving the j split junction and their respective metal concentrations, respectively. The performance of each split junction is defined by a variable, $X(j)_{\text{split}}$, defined as continuous in the [0,1] interval.

Reverse osmosis membrane modules:

$$Q(k)_{\text{memb}} = Q(k)_{\text{perm}} + Q(k)_{\text{ret}} \tag{14}$$

$$Q(k)_{\text{memb}} C(k)^{\text{metal}}_{\text{memb}} = Q(k)_{\text{perm}} C(k)^{\text{metal}}_{\text{perm}} + Q(k)_{\text{ret}} C(k)^{\text{metal}}_{\text{ret}} \tag{15}$$

where $Q(k)_{\text{memb}}$ and $C(k)^{\text{metal}}_{\text{memb}}$ denote the flow of the stream entering the k reverse osmosis membrane module and the corresponding concentration of each metal in the same stream, respectively, $Q(k)_{\text{perm}}$ and $C(k)^{\text{metal}}_{\text{perm}}$ denote the flow of the permeate stream leaving the k membrane module and its respective metal concentrations, respectively, and $Q(k)_{\text{ret}}$ and $C(k)^{\text{metal}}_{\text{ret}}$ denote the flow of the retentate stream leaving the same membrane module and its respective metal concentrations, respectively.

The characteristic variables that describe the performance of each k reverse osmosis stage, namely, the specific permeate flux $J(k)$ and the rejection coefficient of each metal $R(k)^{\text{metal}}$, can be formulated by direct application of the Kedem–Katchalsky equations

$$J(k) = L_{\text{P}}\, \Delta P(k) \tag{16}$$

$$R(k)^{\text{metal}} = \frac{\sigma^{\text{metal}} J(k)}{J(k) + \omega'^{\text{metal}}} \tag{17}$$

where the applied pressure in the k stage is symbolized by $\Delta P(k)$.

Once the membrane transport is defined, the characteristics of the permeate streams (flow and metal concentrations) can be calculated taking into account the membrane area of the corresponding k stage, $A(k)$

$$Q(k)_{\text{perm}} = 86,400 A(k) J(k) \tag{18}$$

$$C(k)^{\text{metal}}_{\text{perm}} = (1 - \text{R}(k)^{\text{metal}}) C(k)^{\text{metal}}_{\text{memb}} \tag{19}$$

Finally, the recovery ratio of each module, Rec(k) can be defined

$$\text{Rec}(k) = \frac{\text{Q}(k)_{\text{perm}}}{\text{Q}(k)_{\text{memb}}} \tag{20}$$

Optimization Procedure

The main objective of the design was to maximize the daily economic profit of the process obtained from the sale of electronic grade hydrogen peroxide produced by the

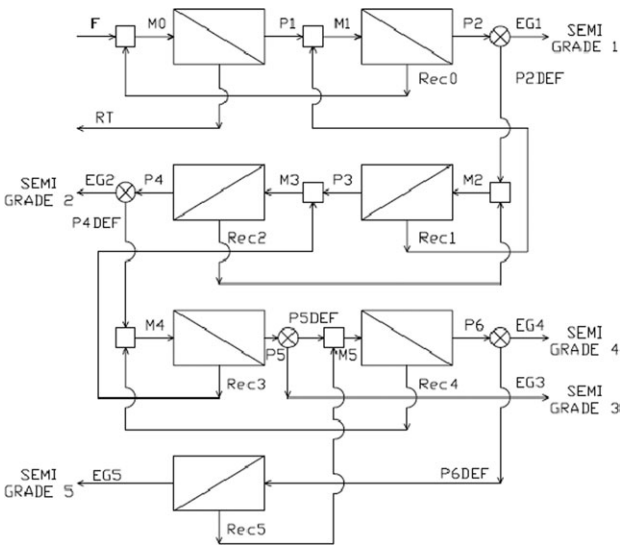

Figure 3. Superstructure configuration.

Table 4. Model Parameters for Calculation

Parameter	Unit	Value
LT_{memb}	d	3
LT_{inst}	d	1825
K_{memb}		0.12
Y_{raw}	$/m^3	790
Y_{EG1}	$/m^3	2592
Y_{EG2}	$/m^3	3537
Y_{EG3}	$/m^3	3780
Y_{EG4}	$/m^3	8721
Y_{EG5}	$/m^3	11826
Y_{memb}	$/m^2	50
Y_{by}	$/m^3	600
Y_{lab}	$/h	7
Y_{elec}	$/(kWh)	0.08
η		0.70
CC_{clean}	$/d	2590

ultrapurification system. A straightforward economic model based on revenues and costs was proposed. The main optimization parameters required are listed in Table 4.

The daily profit (Z) can be expressed as the difference between the total daily revenues of the process (Rev) and the total costs (TC)

$$Z = \text{Rev} - \text{TC} \tag{21}$$

On the one hand, the five different electronic grades of hydrogen peroxide obtainable through the reverse osmosis network contribute to the total revenues of the process, but other output stream of the system, the retentate of the first stage, can also be considered valuable, as it could be commercialized as a by-product useful for hydrogen peroxide applications where metallic content is not a limiting factor. According to this approach, six different terms have to be incorporated to take into account all the contributions implied to assess the total daily revenues

$$\text{Rev} = \text{RT}Y_{\text{by}} + \sum_{n=1}^{5} \text{EG}(n)Y_{\text{EG}(n)} \tag{22}$$

where RT denotes the flow of the first stage retentate stream and Y_{by}, the corresponding price assigned to this by-product stream, EG(n) denotes the flow of the corresponding n SEMI Grade product stream, and $Y_{EG(n)}$, the price of each SEMI Grade hydrogen peroxide.

On the other hand, the total daily costs of the system were calculated by the addition of the capital costs (CC) and the operation costs (OC). The CC attributable to membranes (CC_{memb}) or to the rest of the installation (CCi_{nst}) were differentiated, while the OC were itemized into raw materials (OC_{raw}), energy (OC_{en}), labor (OC_{lab}), and maintenance costs (OC_m)

$$\text{TC} = \text{CC} + \text{OC} \tag{23}$$

$$\text{CC} = \text{CC}_{\text{memb}} + \text{CC}_{\text{inst}} \tag{24}$$

$$\text{OC} = \text{OC}_{\text{raw}} + \text{OC}_{\text{en}} + \text{OC}_{\text{lab}} + \text{OC}_{\text{m}} \tag{25}$$

The CC of the membranes modules considering straight-line depreciation along their lifetime (LT_{memb}) were expressed as function of the total membrane area of the installation

$$\text{CC}_{\text{memb}} = \frac{Y_{\text{memb}}}{\text{LT}_{\text{memb}}} \sum_{k} A(k) \tag{26}$$

where the price of the reverse osmosis membrane elements is symbolized by Y_{memb}.

Once the membranes costs were defined, the CC corresponding to the rest of the installation were related to them by mean of an empirical coefficient (K_{memb}) that expressed the contribution of the investment in membranes to the total CC. The percentage of the total investment attributable to the membranes typically range between 12 and 30%,[61,62] so a value of K_{memb} equal to 0.12 was chosen with the intention of representing the most exigent scenario (an ultrapurification system requires very high-quality and -purity materials)

$$\text{CC}_{\text{ins}} = \text{CC}_{\text{memb}} \frac{(1 - K_{\text{memb}})}{K_{\text{memb}}} \frac{\text{LT}_{\text{memb}}}{\text{LT}_{\text{inst}}} + \text{CC}_{\text{clean}} \tag{27}$$

where LT_{inst} denotes the installation lifetime and CC_{clean}, the CC attributable to the cleanroom. As ultrapurification processes require contamination control, the entire installation need to be included in a cleanroom to provide the necessary controlled atmosphere. The CC attributable to the cleanroom were calculated according to a formula based on the model proposed by Yang and Eng Gan[63]

$$\begin{aligned}\text{CC}_{\text{clean}} = &-1645051 + 5156.6\text{CA} + 68.8\text{MAV} \\ &+ 34\text{EAV} + 2996627\text{AFC} + \text{AN}\end{aligned} \tag{28}$$

where CA refers to the cleanroom area, MAV refers to the make-up air volume, EAV refers to the exhaust air volume, and AFC refers to the average filter coverage ratio. The parameters required by the formulated model for the cost of the cleanroom (Eq. 28) were chosen according to the design of a Class 100 (200 air changes per hour) space of 200 m^2 with raised floor and fan filter unit (FFU) type air ventilation.[64] The term AN, that did not appear in the originally formulated model, was added to include the costs related to analysis and quality control. Its value was assessed according to the research group experience in analytical equipment management, mainly inductively coupled plasma mass spectrometry and ion chromatography.

The OC are essentially based on the consumption of the corresponding resource, except for the case of maintenance costs, which are function of the total CC.[65] The only required raw material was the technical grade hydrogen peroxide used as feed, and the installation was designed to be totally managed by a single worker

$$\text{OC}_{\text{raw}} = \text{FY}_{\text{raw}} \tag{29}$$

$$\text{OC}_{\text{lab}} = 24Y_{\text{lab}} \tag{30}$$

$$\text{OC}_{\text{en}} = \frac{Y_{\text{elec}}}{36\,\eta} \sum_{k} \left(Q(k)_{\text{memb}}\,\Delta P(k)\right) \tag{31}$$

$$\text{OC}_{\text{m}} = 0.05\text{CC} \tag{32}$$

where F denotes the flow of the feed stream, Y_{raw}, the price of the technical grade hydrogen peroxide used as feed raw material, Y_{lab}, the salary assigned to the employee, Y_{elec}, the electricity price, and η, the pump efficiency.

The objective function depends on a large number of quantities that can be separated into variables with respect to

Table 5. Optimization Results

Membrane Stages				Split Junctions		Product Streams	
K	$\Delta P(k)$ (bar)	Rec(k)	$A(k)$ (m^2)	j	$X(j)_{split}$	n	$Q_{EG(n)}$ (m^3/d)
1	40	0.9	14.0	1	1	1	0
2	40	0.9	14.0	2	1	2	0
3	40	0.9	14.0	3	1	3	0
4	40	0.9	14.0	4	1	4	0
5	40	0.9	14.0			5	21.5
6	40	0.9	13.8				
7	40	0.9	12.4				

which the function is maximized and parameters that can be considered as constants during the optimization procedure.

For each reverse osmosis stage, the applied pressure and the recovery ratio were chosen as variables. The investigated ranges of each variable were

$$\Delta P_{min} = 10\text{bar} \leq \Delta P(k) \leq 40\text{bar} = \Delta P_{max} \quad (33)$$

$$\text{Rec}_{min} = 0.3 \leq \text{Rec}(k) \leq 0.9 = \text{Rec}_{max} \quad (34)$$

The configuration of the network is characterized by the split decision variables of each split junctions. The split decision variables are defined in the continuous [0,1] interval (the variable equals to 0, when all the entering flow is derived to the stream leaving the system, and it equals to 1, when the flow is derived to the stream feeding the next stage, whereas intermediate values of the variable imply division of the flow between both streams)

$$X_{\text{split min}} = 0 \leq X(j)_{\text{split}} \leq 1 = X_{\text{split max}} \quad (35)$$

Quality constraints concerning the maximum allowable metallic content in each of the different electronic grade hydrogen peroxide product streams must be taken into account

$$C^{\text{metal}}_{EG(n)} \leq C^{\text{metal}}_{SEMI(n)} \quad (36)$$

where $C^{\text{metal}}_{EG(n)}$ denotes the concentration of each metal in the n SEMI Grade product stream and $C^{\text{metal}}_{SEMI(n)}$ denotes the maximum allowed concentration for each metal in the corresponding n SEMI Grade.

In mathematical terms the optimization model can be expressed as follows

$$\begin{aligned} &\max Z = f(x) \\ &\text{s.t } .h(x) = 0 \\ &\quad w(x) \leq 0 \\ &\quad x \in \Re^n \\ &\quad x_L < x < x_U \end{aligned}$$

being Z the daily profit, x the vector of continuous variables ($\Delta P(k)$, Rec(k), and $X(j)_{split}$), h the vector of equality constraint functions (mass balance and membrane transport equations), and w the vector of inequality constraint functions (product requirements based on the concentration limit for each metallic cation).

Results and Discussion

The installation scale was defined assuming the coupling of the ultrapurification installation to a manufacturing plant with a target annual production aimed to electronic grade purposes of 9000 tons of technical grade hydrogen peroxide. When 330 operating days per year are considered, the corresponding feed flow is above 24 m^3/d. The characterization of the feed stream is based on typical metallic impurities content of technical grade hydrogen peroxide. The feeding conditions (flow and metals concentrations of the feed stream F) are shown in Table 3.

The lifetime of the reverse osmosis membrane in hydrogen peroxide medium (based on the experimental results with BE polyamide membrane from Woongjin Chemical) is notoriously shorter (few days)[19] than the relative one to the most classical applications with seawater or brackish water (some years),[66,67] and the cost of replacement was taken into account in the costs function.

The resulting NLP problem was solved using CONOPT3 solver within the software GAMS. Several starting points were proved to demonstrate the robustness of the solution. In general, a typical run to solve the mathematic programming problem has taken 0.17 central processing unit (CPU) time (s), equivalent to 77 iterations to finish.

Generalized findings

The optimum values that maximize the target function (daily profit Z) of the ultrapurification process were identified by run of the corresponding NLP problem within GAMS software. The results of the optimized configuration are compiled in Table 5.

It was found that the optimum applied pressures for all the stages were 40 bar, which is the upper boundary restriction for these variables. In a similar way, the optimum recovery rates were limited by the upper limit of the defined range (0.9). The optimum system configuration (Figure 4) corresponded to the one that only produce SEMI Grade 5 product stream (all the split junction variables equal to 1 which implies no output of intermediate Grades). Under these conditions, the daily profit could attains 232,170 \$/d, equivalent to an annual profit of 76.6 mill\$.

The main cost of the system was the acquisition the raw material that represented more than 80% of the TC (Figure 5). The rest of the operational costs became insignificant

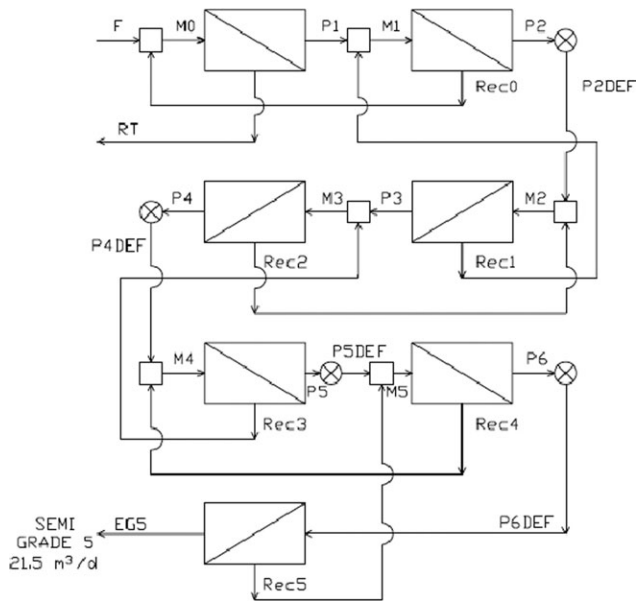

Figure 4. Optimal process configuration.

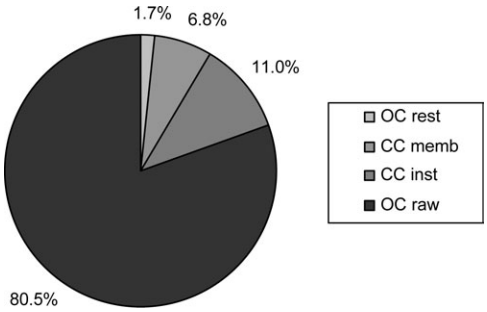

Figure 5. Costs breakdown for the optimum configuration.

when compared to the cost corresponding to feed hydrogen peroxide as none of them attained individually the 1% (they contribute jointly only by 1.7%). On the other hand, when focusing on the CC, the investment on membranes contributes by no more than 7% to the TC despite the high replacement rate consequence of the short membrane lifetime in such an oxidant medium.

Previous results, corresponding to optimization of ultrapurification cascade systems with increasing number of stages (from two to seven stages), had demonstrated that production of the most exigent electronic grades was more profitable despite the higher number of stages than the least strict grades.[60] This fact can be explained by the great influence of the market prices of the different Grades: SEMI Grade 5 is much more valuable than SEMI Grade 1 (four times more expensive as seen in Table 4), but the TC of the installation required to produce Grade 5 (seven stages) is only less than 6% higher than the corresponding to Grade 1 manufacturing (two stages). So the optimum results of the superstructure configuration confirm the trend to promote the production of higher quality hydrogen peroxide.

The characteristics of the product stream (impurities content) for the optimally configured system are listed in Table 6. As expected, all the metallic concentrations felt below the limit of 10 ppt. The limiting solute is the Na, because its concentration (0.747 ppt) is the highest among all the impurities but still quite lower than the bound fixed by SEMI. To quantify in an easier way the product quality when compared to the requirements, a safety factor (SF) was defined according to Eq. 37

$$SF_n = \frac{C^{metal}_{SEMI(n)}}{C^{metal}_{EG(n)}} = \frac{\text{Failure concentration}}{\text{Design concentration}} \qquad (37)$$

where the SF is represented as the ratio between the failure and design concentrations (in this case the maximum allowed concentration divided by the product concentration). Now, it can be said that Na is the limiting impurity in terms of SFs, as it has the lowest value. Anyway, a value equal to 13 for the SF is a common figure when compared to commercially available electronic grade hydrogen peroxides.

Effect of market restrictions

As aforementioned, the process economy invited to stimulate the production of the strictest grade hydrogen peroxide, but market restrictions may represent the counterpoint to this situation. It seems more reasonable to expect that the demand of the most exigent Grade 5 would be limited, not allowing the commercialization of all the output obtained under a "produce the highest quality Grade as much as possible" strategy. This proposed realistic framework would include also some commitments acquired with the corresponding clients to serve them with products others than the strictest Grade 5 (only required for very exigent tasks during the manufacturing of semiconductor materials and microelectronic devices and replaceable by lower quality product for the rest of productive steps).

Therefore, three different scenarios (Scenarios 1–3) were initially projected to represent more realistic commercial situations to investigate the influence of market restrictions over the configuration of the ultrapurification process. The scenarios were defined by a minimum and a maximum flow for each of the grades (Table 7).

The Scenario 1 represents the market baseline: production limitations are just imposed by both low and upper bounds. On the one hand, at least a minimum production of each grade has to be obtained to fulfill obligations acquired with consumers. On the other hand, there is a maximum production for each grade that can be absorbed by the demand. The Scenarios 2 and 3 consider the high- and low-demand circumstances respectively. In each situation, both minimum and maximum restrictions are increased or decreased if compared with the baseline Scenario 1.

The optimization results of the different basic scenarios are given in Table 8. Again, all the optimum values of the design and operation variables coincided with the defined upper bounds (0.9 for the recovery rates and 40 bar for the applied pressures, respectively) whichever scenario is observed. The profits of the three proposed scenarios were severely reduced when compared with the ideal situation without market restrictions: the highest drop corresponded to the low-demand Scenario 3 (61%) and the lowest discount to the baseline Scenario 1 (40%), remaining the high-demand Scenario 2 in an intermediate situation with 54% reduction. The main reason of the reduced profit was the lower revenues of the system related with commercialization of less valuable products, because the TC of the restricted scenarios were also reduced (but not in a relevant way, as the highest decrease corresponding to Scenario 3 is only 2%, not comparable with the 55% cut in the revenues of the same scenario).

When paying attention to the system configuration, Scenario 1 was characterized by just achievement of the minimum demands for the least exigent Grades 1–3; Grade 5 stream equal to its maximum allowed bound; and the rest of the production leaving the system as Grade 4 hydrogen peroxide. The high-demand Scenario 2 could be expected to be more profitable that the baseline demand scenario (higher total demand). But the results showed that the Scenario 1

Table 6. Impurities Content of the Product Stream for the Optimum Configuration

	C_{EG5} (ppt)	SF_5
B	0.353	28
Na	0.747	13
Al	0.085	118
Ti	0.012	864
Cr	0.009	1152
Mn	0.001	9566
Fe	0.164	61
Ni	0.002	4088
Cu	<0.001	>10000
Zn	0.002	5085

Table 7. Flow Restrictions of Each Product Stream Under the Different Marketing Scenarios

	Flow Restrictions to Product Streams (m^3/d)									
	SEMI Grade 1		SEMI Grade 2		SEMI Grade 3		SEMI Grade 4		SEMI Grade 5	
Scenario	Q_{EG1min}	Q_{EG1max}	Q_{EG2min}	Q_{EG2max}	Q_{EG3min}	Q_{EG3max}	Q_{EG4min}	Q_{EG4max}	Q_{EG5min}	Q_{EG5max}
1	2	30	1	3	5	30	2	10	1	5
2	4	40	2.5	9	7	38	3.7	18	1.9	8
3	1	14	0.6	1.3	2	12	0.8	3.6	0.6	2.1
4	4	40	2.5	9	7	38	0.8	3.6	0.6	2.1
5	1	14	0.6	1.3	2	12	3.7	18	1.9	8

was more satisfactory in economic terms. The Scenario 2 was defined by minimum productions of every Grades but Grade 5. Under these conditions, the main part of the raw material had to be used to fulfill the requirements of the least profitable grades, remaining few resources to be assigned to the most valuable grades. The Scenario 3 is just the opposite case: the low-demand restrictions implied that all the grades except Grade 1 were produced in their maximum amounts. Anyway, as these limits are quite lower than the ones corresponding to the baseline situation, the profit of the system fell down (in this case because the low demand of the high-valuable Grades forced to spend most of the raw material in the least profitable Grade 1).

In light of the results obtained for the basic market restrictions, two new scenarios were proposed for consideration: the Scenarios 4 and 5 corresponded to mixed demand situations. The Scenario 4 included the high-demand conditions for Grades 1–3 (as in Scenario 2) and the low-demand conditions for Grades 4 and 5 (as in Scenario 3). In a reverse way, the Scenario 5 covered the low-demand limits for Grades 1–3 (corresponding to Scenario 3) and the high-demand values for Grades 4 and 5 (as in Scenario 2).

The optimization results of the different mixed demand scenarios are shown in Table 9. Once again, all the optimum values of the design and operation variables coincided with the defined upper bound for both scenarios. The economic aspects of the different scenarios are compiled in Table 10. As expected, the Scenario 4 was the least profitable one, because it joined two undesirable factors: high demand of less valuable grades and low demand of the preferred high-quality grades. This combination implied an unbalanced distribution of the resources between both types of grades, converting the low-quality ones into the predominant products. On the other hand, Scenario 5 represented also out of balance market conditions, but in this case as the more valuable Grades became dominant, the economic profit of the corresponding system configuration reached a value better than the baseline Scenario 1 (23% of extra profit). The main results of the optimization of the different scenarios restricted by market conditions are depicted in Figure 6.

By way of guidance, the quality characteristics of the different grades obtained under the Scenario 1 conditions are listed in Table 11. It can be observed that Na is the limiting impurity whichever considered grade as the corresponding SFs are the lowest ones. However, all the SFs are higher than 5, so no problems could be expected, even under some uncertainty conditions about the metallic content of the raw material or the performance of the membrane modules. After comparison of the dated included in Table 11 with those of the Table 6 (corresponding to the ideal situation without market restriction), it can be concluded that the ideal situation obtained a higher quality SEMI Grade 5 hydrogen peroxide. This result can be explained by the assignment of material out of the system to the production of intermediate

Table 8. Optimization Results for the Basic Marketing Scenarios

Membrane Stages				Split Junctions		Product Streams	
k	$\Delta P(k)$ (bar)	Rec(k)	$A(k)$ (m^2)	j	$X(j)_{split}$	n	$Q_{EG(n)}$ (m^3/d)
Scenario 1							
1	40	0.9	14.0	1	0.916	1	2.0
2	40	0.9	13.9	2	0.954	2	1.0
3	40	0.9	12.7	3	0.751	3	5.0
4	40	0.9	12.6	4	0.395	4	8.5
5	40	0.9	11.6			5	5.0
6	40	0.9	8.1				
7	40	0.9	2.9				
Scenario 2							
1	40	0.9	14.0	1	0.831	1	4.0
2	40	0.9	13.7	2	0.870	2	2.5
3	40	0.9	11.4	3	0.561	3	7.0
4	40	0.9	11.1	4	0.564	4	3.7
5	40	0.9	9.2			5	4.3
6	40	0.9	4.9				
7	40	0.9	2.5				
Scenario 3							
1	40	0.9	14.0	1	0.895	1	2.5
2	40	0.9	13.8	2	0.938	2	1.3
3	40	0.9	12.3	3	0.346	3	12.0
4	40	0.9	12.2	4	0.393	4	3.6
5	40	0.9	10.6			5	2.1
6	40	0.9	3.4				
7	40	0.9	1.2				

Table 9. Optimization Results for the Mixed Demand Marketing Scenarios

Membrane stages				Split junctions		Product streams	
k	$\Delta P(k)$ (bar)	Rec(k)	$A(k)$ (m^2)	j	$X(j)_{split}$	n	$Q_{EG(n)}$ (m^3/d)
Scenario 4							
1	40	0.9	14.0	1	0.831	1	4.0
2	40	0.9	13.7	2	0.870	2	2.5
3	40	0.9	11.4	3	0.406	3	9.3
4	40	0.9	11.1	4	0.393	4	3.6
5	40	0.9	9.1			5	2.1
6	40	0.9	3.4				
7	40	0.9	1.2				
Scenario 5							
1	40	0.9	14.0	1	0.958	1	1.0
2	40	0.9	13.9	2	0.974	2	0.6
3	40	0.9	13.3	3	0.909	3	2.0
4	40	0.9	13.3	4	0.473	4	9.9
5	40	0.9	12.7			5	8.0
6	40	0.9	10.9				
7	40	0.9	4.6				

Table 10. Economic Breakdown of the Different Scenarios

Economic Terms (mill$/y)	No Market Restrictions	Market Scenario 1	Market Scenario 2	Market Scenario 3	Market Scenario 4	Market Scenario 5
Z	76.616	45.928	35.407	30.057	29.399	56.555
Rev	84.445	53.636	43.062	37.717	37.037	64.305
TC	7.829	7.708	7.655	7.660	7.638	7.750
CC	1.390	1.276	1.227	1.231	1.210	1.315
CC_{memb}	0.529	0.417	0.368	0.372	0.351	0.455
CC_{inst}	0.861	0.860	0.859	0.859	0.859	0.860
OC	6.439	6.432	6.428	6.429	6.427	6.434
OC_{raw}	6.306	6.306	6.306	6.306	6.306	6.306
OC_{lab}	0.055	0.055	0.055	0.055	0.055	0.055
OC_{en}	0.008	0.006	0.005	0.005	0.005	0.007
OC_m	0.070	0.064	0.061	0.062	0.061	0.066

grades instead of allowing it to be recirculated to previous stages, improving the quality of the streams leaving the mixers because of the input of higher fluxes of recirculated streams with lower metallic content.

A second optimization problem was also formulated and solved to investigate the effects of the different market restrictions. In this case, the objective was the minimization of the TC of the system corresponding with the situations where all the demand of each scenario can be satisfied (Scenarios 1–3 Full). In order to be able to assure the total demand, the feed stream of the system was not previously fixed, and it was set as another variable of the system.

In mathematical terms this new optimization problem can be expressed as follows

$$\begin{aligned} &\min \mathrm{TC} = f(x) \\ &\text{s.t.} h(x) = 0 \\ &\quad w(x) \le 0 \\ &\quad x \in \Re^n \\ &\quad x_L < x < x_U \end{aligned}$$

being x the vector of continuous variables (F, $\Delta P(k)$, Rec(k), and $X(j)_{split}$), h the vector of equality constraint functions (mass balance and membrane transport equations), and w the vector of inequality constraint functions (product requirements).

Once again, the optimum applied pressures resulted 40 bar for all the stages (upper boundary restriction). In a similar way, the optimum recovery rates were limited by the upper limit of the defined range (0.9). These results showed that minimization of TC and maximization of economic profit led to the same optimum solutions.

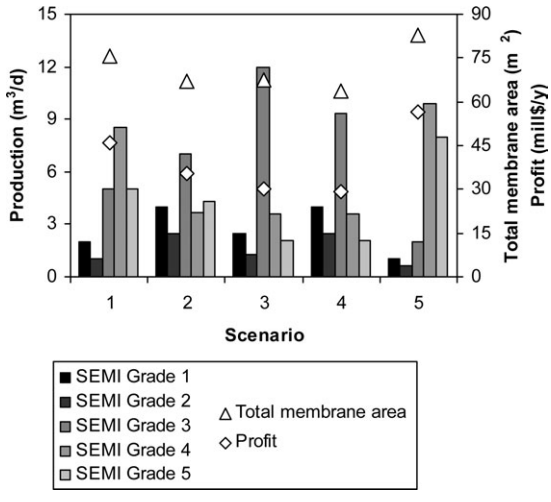

Figure 6. Main results of the optimization of the different scenarios under market restrictions.

The optimization results of the different fully satisfied scenarios are listed in Table 12, and the corresponding economic breakdown can be observed in Table 13. Under these conditions, the raw material required by the system is much greater than the original baseline: the high-demand Scenario 2 Full consumed more than five times the baseline feed flow (127.1 m^3/d vs. 24.2 m^3/d). On the other hand, the higher consumption of technical grade hydrogen peroxide was compensated with greater profits. As an example, the Scenario 1 Full is approximately twice more profitable than the Scenario 1. Another result worth mentioning is the comparison of the three fully satisfied Scenarios. The Scenario 2 Full, related with high-demand patterns, is more profitable than the Scenario 1 Full (corresponding with baseline demand). When the feed stream flow was limited, the Scenario 1 was more favorable than the Scenario 2 as the high demand of low-price grades limited the production of Grades 4 and 5. Without feed restrictions, the limitations disappeared, and the Scenario 2 Full became the most lucrative. Anyway, the Scenario 3 Full appeared again as the least beneficial one because of its low-demand framework.

Effect of unit costs

All the previous optimization results demonstrated a very robust performance of the system, as the variables had acquired the maximum allowed value in the corresponding range in every case. A simple sensitivity analysis was carried out to advance in the investigation of the influence of the parameters governing the costs associated with the main design and operation variables: the electricity unit price influences the energy costs attributable to the pressurization of the

Table 11. Impurities Contents of the Product Streams for the Optimum Configuration Under Scenario 1 Conditions

	SF_1	SF_2	SF_3	SF_4	SF_5
B	213	370	167	100	32
Na	6	8	10	11	13
Al	87	99	100	111	116
Ti	338	1000	1000	910	859
Cr	80	1429	1314	1228	1147
Mn	806	>10000	>10000	>10000	9566
Fe	27	149	111	100	62
Ni	177	3333	3870	3957	4031
Cu	6250	>10000	>10000	>10000	>10000
Zn	617	5000	5504	5276	5049

Table 12. Optimization Results (Minimum TC) for the Full Satisfied Marketing Scenarios

Membrane Stages		Split Junctions		Product Streams		Feed Stream
K	$A(k)$ (m^2)	j	$X(j)_{split}$	N	$Q_{EG(n)}$ (m^3/d)	F (m^3/d)
Scenario 1 Full						
1	50.5	1	0.643	1	30.0	87.7
2	48.6	2	0.944	2	3.0	
3	31.2	3	0.358	3	30.0	
4	30.8	4	0.357	4	10.0	
5	27.0			5	5.0	
6	9.0					
7	2.9					
Scenario 2 Full						
1	73.2	1	0.672	1	40.0	127.1
2	70.7	2	0.888	2	9.0	
3	47.4	3	0.433	3	38.0	
4	46.6	4	0.331	4	18.0	
5	38.8			5	8.0	
6	15.6					
7	4.6					
Scenario 3 Full						
1	21.4	1	0.604	1	14.0	37.1
2	20.5	2	0.938	2	1.3	
3	12.3	3	0.346	3	12.0	
4	12.2	4	0.393	4	3.6	
5	10.6			5	2.1	
6	3.4					
7	1.2					

streams entering the reverse osmosis modules, and the membrane unit price controls the membrane costs related to the total membrane area of each stage. In each case, the available membrane area defines the quantity of permeate obtained by each stage and, consequently, the recovery ratio of them. Besides, the membrane costs are used as the basis to calculate the rest of the CC and even the maintenance costs are related with the total CC.

Table 13. Economic Breakdown of the Different Full Satisfied Scenarios

Economic Terms (mill$/y)	Market Scenario 1 Full	Market Scenario 2 Full	Market Scenario 3 Full
TC	25.003	35.837	11.109
CC	1.968	2.507	1.309
CC_{memb}	1.100	1.633	0.449
CC_{inst}	0.868	0.874	0.860
OC	23.034	33.330	9.800
OC_{raw}	22.864	33.125	9.673
OC_{lab}	0.055	0.055	0.055
OC_{en}	0.016	0.024	0.007
OC_m	0.098	0.125	0.065
Rev	116.798	177.928	47.830
Z	91.795	142.091	36.720

The sensitivity analysis results (Table 14) showed that the total profit of the system under Scenario 1 conditions is very insensitive to changes in electricity, membrane, and raw material unit prices. The optimum values of the variables resulted again at the upper bounds (0.9 and 40 bar). The variations in the profit were located in the range $\pm 1\%$ even for changes in an order of magnitude in the price of the electricity or when the membrane price was doubled. As the raw material is the main cost of the system, the influence of its unitary cost is higher than those of the other costs, but the revenues are so dominant that a decrease or increase of 20% in the price of the feed only affect in the range $\pm 3\%$ to the economic profit of the process.

To confirm the robustness of the optimum values for the design and operation variables, a search of such conditions that would modify the optimal solution was planned out. For the case of applied pressures, the electricity unit price of 6 \$/kW h would move the optimum value for the applied pressures from the upper bound to 39.4 bar for every stages under Scenario 1 conditions. Such a high-expensive electricity situation seems very improbable, because it would require a nearly 100-fold increase in the price of the energy. A quite similar result was obtained after exploration of conditions for different optimal recovery rates: very expensive reverse osmosis membranes (6000 \$/m^2) would move the optimal recovery rate of the first stage to 0.647 (but none of the rest of stages). Again, an approximately 100-fold raise in membranes prices cannot be considered as a logic panorama; and in the case it could happen, the process would not be longer economically viable.

Conclusions

The proposed superstructure represents a seven-stage countercurrent cascade system able to produce simultaneously all the different SEMI grades, from two stages corresponding to SEMI Grade 1, to seven stages that are required for SEMI Grade 5, the strictest grade related to the metal impurities.

The objective of the design was to maximize the daily profit obtained from the sale of the electronic grades of hydrogen peroxide produced by the ultrapurification system, calculated as the difference between the total daily revenues and the TC (capital and operation).

The obtained results allow to conclude with the viability of the ultrapurification process based on the reverse osmosis modules, with the optimum system configuration that only produce SEMI Grade 5 hydrogen peroxide (the strictest grade, high-value product) as the best option in economic terms when there are no market restrictions: 232,170 \$/day, equivalent to an

Table 14. Sensitivity Analysis for Electricity, Membrane, and Technical Grade Hydrogen Peroxide Unit Prices

	Electricity price (\$/(kW h))			Membrane price (\$/m^2)			Technical grade hydrogen peroxide price (\$/m^3)		
Economic terms (mill$/y)	0.02	0.08	0.80	10	50	100	632	790	948
CC_{memb}				0.083	0.417	0.833			
CC_{inst}				0.856	0.860	0.865			
OC_m				0.047	0.064	0.085			
OC_{en}	0.002	0.006	0.061						
OC_{raw}							5.045	6.306	7.568
Z	45.933	45.928	45.873	46.282	45.928	45.486	47.189	45.928	44.667
Z variation (%)	+0.01		−0.12	0.77		−0.96	+2.75		−2.75

annual profit of 76.6 mill$ (for a plant capacity of 9000 tons/year of technical grade hydrogen peroxide).

The main cost of the system was the raw material that represents more than 80% of the TC. The investment on membranes contributes by no more than 7% to the CC, despite the high replacement rate due to the membrane lifetime in such and oxidant medium.

The influence of market restrictions was studied under different scenarios, given in terms of production of each SEMI Grade hydrogen peroxide, taking into account that the strictest Grade 5 may be only required for very exigent tasks during the manufacturing of semiconductor materials. The economic profit of the system configuration reached a value better than the baseline scenario in the scenario that represents the dominance of the more valuable Grades 4 and 5, with 23% of extra profit mainly given by the high market price of these demanded electronic grades.

The effect of unit costs was analyzed in terms of electricity, membrane, and raw material unit prices showing that the total profit of the system is very insensitive to changes, being remarked the key factor of the market prices of the electronic grades of hydrogen peroxide.

Acknowledgments

This research has been financially supported by the Ministry of Science and Innovation of Spain (MICINN) through CTM2006-00317 and CTQ2010-16608 Projects. R. Abejón acknowledges also the assistance of MICINN for the award of a FPI grant (BES-2008-003622).

Notation

$A(k)$ = membrane area of the k stage, m^2
AFC = average filter coverage ratio
AN = capital costs attributable to analysis and quality control, $
CA = cleanroom area, m^2
CC = capital costs, $/d
CC_{clean} = capital costs attributable to cleanroom, $/d
CC_{inst} = capital costs attributable to installation, $/d
CC_{memb} = capital costs attributable to membranes, $/d
C_F = solute feed concentration, mol/m^3
$C(i)^{metal}_{mixin1}$ = metal concentration of the first stream entering the i mixer, ppb
$C(i)^{metal}_{mixin2}$ = metal concentration of the second stream entering the i mixer, ppb
$C(i)^{metal}_{mixout}$ = metal concentration of the output stream leaving the i mixer, ppb
$C(j)^{metal}_{splitin}$ = metal concentration of the stream entering the j split junction, ppb
$C(j)^{metal}_{splitout1}$ = metal concentration of the stream leaving the j split junction to the next stage, ppb
$C(j)^{metal}_{splitout2}$ = metal concentration of the stream leaving the j split junction out of the system, ppb
$C(k)^{metal}_{memb}$ = metal concentration of the stream entering the k membrane stage, ppb
$C(k)^{metal}_{perm}$ = metal concentration of the permeate stream leaving the k membrane stage, ppb
$C(k)^{metal}_{ret}$ = metal concentration of the retentate stream leaving the k membrane stage, ppb
C_P = solute permeate concentration, mol/m^3
$(C_S)_{ln}$ = logarithmic average solute concentration across the membrane, mol/m^3
EAV = exhaust air volume, m^3/h
EG(n) = flow of the corresponding n SEMI Grade product stream, m^3/d
i = van 't Hoff factor
$J(k)$ = permeate flux of the k membrane stage, m/s
J_S = solute flux, mol/m^2 s
J_V = solvent flux, m/s
K_A = dissociation constant, M
K_{memb} = ratio membrane capital costs to total capital costs
L_P = solvent permeability coefficient, m/s bar
LT_{memb} = membrane lifetime, d
LT_{inst} = installation lifetime, d
m = solute molar concentration, $(mol/m^3$
MAV = make-up air volume, m^3/h
OC = operation costs, $/d
OC_{en} = energy costs, $/d
OC_{lab} = labor costs, $/d
OC_m = maintenance costs, $/d
OC_{raw} = raw material costs, $/d
$Q(i)_{mixin1}$ = flow of the first stream entering the i mixer, m^3/d
$Q(i)_{mixin2}$ = flow of the second stream entering the i mixer, m^3/d
$Q(i)_{mixout}$ = flow of the output stream leaving the i mixer, m^3/d
$Q(j)_{splitin}$ = flow of the stream entering the j split junction, m^3/d
$Q(j)_{splitout1}$ = flow of the stream leaving the j split junction to the next stage, m^3/d
$Q(j)_{splitout2}$ = flow of the stream leaving the j split junction out of the system, m^3/d
$Q(k)_{memb}$ = flow of the stream entering the k membrane stage, m^3/d
$Q(k)_{perm}$ = flow of the permeate stream leaving the k membrane stage, m^3/d
$Q(k)_{ret}$ = flow of the retentate stream leaving the k membrane stage, m^3/d
R = rejection coefficient
$\Re$ = gas constant, bar m^3/K mol
$R(k)^{metal}$ = rejection coefficient of the corresponding metal in the k stage
Rec(k) = recovery rate of the k stage
Rev = daily revenues, $/d
RT = flow of the first stage retentate stream, m^3/d
T = temperature, K
TC = total costs, $/d
x_F = feed hydrogen peroxide concentration, M
x_P = permeate hydrogen peroxide concentration, M
$X(j)_{split}$ = decision variable of the j split junction
Y_{by} = price of by-product hydrogen peroxide from first stage retentate, $/m^3$
$Y_{EG(n)}$ = price of n SEMI Grade hydrogen peroxide, $/m^3$
Y_{elec} = electricity price, $/(kW h)
Y_{lab} = salary, $/h
Y_{memb} = price of reverse osmosis membranes, $/m^2$
Y_{raw} = price of technical grade hydrogen peroxide, $/m^3$
Z = daily profit, $/d

Greek letters

ΔP = pressure difference across the membrane, bar
$\Delta P(k)$ = applied pressure difference in the k membrane stage, bar
$\Delta\Pi$ = osmotic pressure difference across the membrane, bar
η = pump efficiency
v = stoichiometric coefficient based on van 't Hoff factor
Π = osmotic pressure, bar
σ = reflection coefficient
σ^{metal} = reflection coefficient of the corresponding metal
ω = coefficient of solute mobility, $mol/(m^2$ s bar)
ω' = modified coefficient of solute mobility, m/s
ω'^{metal} = modified coefficient of solute mobility of the corresponding metal, m/d

Indexes

i = number of mixers
j = number of split junctions
k = number of membrane stages
n = number of SEMI Grades

Literature Cited

1. Davison JB, Hoffman JG, Yuan WI. *Ultrapurification of semiconductor process liquids.* In: 9th ICCCS Proceedings, Los Angeles, CA, Sept. 26-30,1988.
2. Reinhardt K, Kern W. *Handbook of Silicon Wafers Cleaning Technology*. Norwich: Wiiliam Andrew, Inc., 2008.
3. Sievert WJ. A European perspective on electronic chemicals. *Semicond Fabtech*. 2000;10:199–204.
4. Kern W, Puotinen D. Cleaning solutions based on hydrogen for use in silicon semiconductor technology. *RCA Rev*. 1970;31:187–206.
5. Freedonia Group. Electronic chemicals to 2008. Industry Study No. 1852, 2004.

6. Olson ED, Reaux CA, Ma WC, Butterbaugh JW. Alternatives to standard wet cleans. *Semicond Int*. 2000;23:70–75.
7. The Engineer. Electrolysed acid strips for semiconductors, March 2007 (Online version).
8. Jeon JS, Ogle B, Baeyens M, Mertens P. Evaluation of cleaning recipes based on ozonated water for pre-gate oxide cleaning. *Solid State Phenom*. 1999;65–66:119–122.
9. Sohn HS, Butterbaugh JW, Olson ED, Diedrick J, Lee NP. Using cost-effective dilute acid chemicals to perform postetch interconnect cleans. *MICRO*. 2005;23:67–76.
10. Rath DL, Ravikumar R, Delehanty DJ, Filippi RG, Kiewra EW, Stojakovic G, McCullough KJ, Miura DD, Rhoads BN. New aqueous clean for aluminum interconnects: Part I. Fundamentals. *Solid State Phenom*. 2001;76–77:31–34.
11. Ravikumar R, Rath DL, Delehanty DJ, Filippi RG, Kiewra EW, Stojakovic G, McCullough KJ, Miura DD, Gambino J, Schnabel F, Rhoads BN. New aqueous clean for aluminum interconnects: Part II. Applications. *Solid State Phenom*. 2001;76–77:51–54.
12. Archer L, Henry SA, Nachreiner D. Removing postash polymer residue from BEOL structures using inorganic chemicals. *MICRO*. 2001;6:95–103.
13. Couteau T, Dawson G, Halladay J, Archer L. Comparing single-wafer and batch polymer cleans using inorganic chemicals in BEOL applications. *MICRO*. 2006;24:45–49.
14. Semiconductor Equipment and Materials International (SEMI). Specifications for hydrogen peroxide. SEMI Document C30-1110, 2010.
15. Goor G, Glenneberg J, Jacobi S. *Hydrogen peroxide*. In: *Ullmann's Encyclopedia of Industrial Chemistry*. Weinheim: Wiley-VCH, 2007 (Electronic release).
16. Sievert WJ. Setting standards—The developments of standards in the field of electronic chemicals. *Semicond Fabtech*. 2001;13:175–179.
17. Abejón R, Garea A, Irabien A. Ultrapurification of hydrogen peroxide solution from ionic metals impurities to semiconductor grade by reverse osmosis. *Sep Purif Technol*. 2010;76:44–51.
18. Caus A, Braeken L, Boussu K, Van der Bruggen B. The use of integrated countercurrent nanofiltration cascades for advanced separations. *J Chem Technol Biotechnol*. 2009;84:391–398.
19. Abejón R, Garea A, Irabien A. Analysis, modelling and simulation of hydrogen peroxide ultrapurification by multistage reverse osmosis. *Chem Eng Res Des*. 2012;90 (doi:10.1016/j.cherd.2011.07.025).
20. Fritzmann C, Löwenberg J, Wintgens T, Melin T. State-of-the-art of reverse osmosis desalination. *Desalination*. 2007;216:1–76.
21. Aboabboud M, Elmasallati S. Potable water production from seawater by the reverse osmosis technique in Libya. *Desalination*. 2007;203:119–133.
22. Park C, Park PK, Mane PP, Hyung H, Gandhi V, Kim SH, Kim JH. Stochastic cost estimation approach for full-scale reverse osmosis desalination plants. *J Membr Sci*. 2010;364:52–64.
23. Peñate B, García-Rodríguez L. Retrofitting assessment of the Lanzarote IV seawater reverse osmosis desalination plant. *Desalination*. 2011;266:244–255.
24. Voutchkov N. Overview of seawater concentrate disposal alternatives. *Desalination*. 2011;273:205–219.
25. Geraldes V, Semiãoa V, de Pinhoa N. Optimization of ladder-type spacers for nanofiltration and reverse osmosis spiral-wound modules by computational fluid dynamics. *Comput Aided Chem Eng*. 2004;18:187–192.
26. Senthilmurugan S, Gupta SK. Modeling of a radial flow hollow fiber module and estimation of model parameters for aqueous multi-component mixture using numerical techniques. *J Membr Sci*. 2006;279:466–478.
27. Fujiwara N, Matsuyama H. The analysis and design of a both open ended hollow fiber type RO module. *J Appl Polym Sci*. 2008;110: 2267–2278.
28. Johnson J, Busch M. Engineering aspects of reverse osmosis module design. *Desalination Water Treat*. 2010;15:236–248.
29. Mo H, Ng HY. An experimental study on the effect of spacer on concentration polarization in a long channel reverse osmosis membrane cell. *Water Sci Technol*. 2010;61:2035–2041.
30. Kostoglou M, Karabelas AJ. Mathematical analysis of the mesoscale flow field in spiral-wound membrane modules. *Ind Eng Chem Res*. 2011;50:4653–4666.
31. Maskan F, Wiley DE, Johnston LPM, Clements DJ. Optimal design of reverse osmosis module networks. *AIChE J*. 2000;46:946–954.
32. Wilf W, Klinko K. Optimization of seawater RO systems design. *Desalination*. 2001;138:299–306.
33. Villafafila A, Mujtaba IM. Fresh water by reverse osmosis based desalination: simulation and optimisation. *Desalination*. 2003;155: 1–13.
34. Glueckstren P, Priel M. Optimization of boron removal in old and new SWRO systems. *Desalination*. 2003;156:219–228.
35. Wilt M, Bartels C. Optimization of seawater RO systems design. *Desalination*. 2005;173:1–12.
36. Avlonitis SA. Optimization of the design and operation of seawater RO desalination plants. *Sep Sci Technol*. 2005;40:2663–2678.
37. Guria C, Bhattacharya PK, Gupta SK. Multi-objective optimization of reverse osmosis desalination units using different adaptations of the non-dominated sorting genetic algorithm (NSGA). *Comput Chem Eng*. 2005;29:1977–1995.
38. Lu YY, Hu YD, Zhang XL, Wu LY, Liu QZ. Optimum design or reverse osmosis system under different feed concentration and product specification. *J Membr Sci*. 2007;287:219–229.
39. Gilau AM, Small MJ. Designing cost-effective seawater reverse osmosis system under optimal energy options. *Renew Energy*. 2008;33:617–630.
40. Vince F, Marechal F, Aoustin E, Bréant P. Multi-objective optimization of RO desalination plants. *Desalination*. 2008;222:96–118.
41. Zhu A, Christofides PD, Cohen Y. Minimization of energy consumption for a two-pass membrane desalination: effect of energy recovery, membrane rejection and retentate recycling. *J Membr Sci*. 2009;339:126–137.
42. Zhu A, Rhardianto A, Christofides PD, Cohen Y. Reverse osmosis desalination with high permeability membranes—cost optimization and research needs. *Desalination Water Treat*. 2010;15:256–266.
43. Li M. Minimization of energy in reverse osmosis water desalination using constrained nonlinear optimization. *Ind Eng Chem Res*. 2010;49:1822–1831.
44. Sassi KM, Mujtaba IM. Optimal design and operation of reverse osmosis desalination process with membrane fouling. *Chem Eng J*. 2011;171:582–593.
45. El-Halwagi MM, Mahmoud M. Synthesis of reverse osmosis networks for waste reduction. *AIChE J*. 1992;38:1185–1198.
46. Voros NG, Maroulis ZB, Marinos-Kouris D. Optimization of reverse osmosis networks for seawater desalination. *Comput Chem Eng*. 1996;20:345–350.
47. González MP, Navarro R, Saucedo I, Avila M, Revilla J, Bouchard C. Purification of phosphoric acid solutions by reverse osmosis and nanofiltration. *Desalination*. 2002;147:315–320.
48. Kulkarni A, Mukherjee D, Mukherjee D, Gill WN. Reprocessing hydrofluoric acid etching solutions by reverse osmosis. *Chem Eng Commun*. 1994;129:53–68.
49. Eul W, Moeller A, Steiner N. *Hydrogen peroxide*. In: *Kirk-Othmer Encyclopedia of Chemical Technology*. New York: Wiley-VCH, 2001 (Electronic release).
50. Soltanieh M, Gill WN. Review of reverse osmosis membranes and transport models. *Chem Eng Commun*. 1981;12:279–363.
51. Kedem O, Katchalsky A. Thermodynamic analysis of the permeability of biological membranes to non-electrolytes. *Biochim Biophys Acta*. 1958;27:229–246.
52. Gupta SK. Design and analysis of reverse osmosis systems using three parameter models for transport across the membrane. *Desalination*. 1992;85:283–296.
53. Van Gauwbergen D, Baeyens J. Modelling reverse osmosis by irreversible thermodynamics. *Sep Purif Technol*. 1998;13:117–128.
54. Tu KL, Nghiem LD, Chivas AR. Boron removal by reverse osmosis membranes in seawater desalination applications. *Sep Purif Technol*. 2010;75:87–101.
55. Bhattacharjee C, Sarkar P, Datta S, Gupta BB, Bhattacharya PK. Parameter estimation and performance study during ultrafiltration of Kraft black liquor. *Sep Purif Technol*. 2006;51:247–257.
56. Kovács Z, Discacciati M, Samhaber W. Modeling of amino acid nanofiltration by irreversible thermodynamics. *J Membr Sci*. 2009;332:38–49.
57. Prabhavathy C, De S. Estimation of transport parameters during ultrafiltration of pickling effluent from a tannery. *Sep Sci Technol*. 2010;45:11–20.
58. Pusch W. Determination of transport parameters of synthetic membranes by hyperfiltration experiments, Part I: Derivation of transport relationship from linear relations of thermodynamics of irreversible processes. *Ber Bunsen Phys Chem*. 1977;81:269–276.
59. Pusch W. Determination of transport parameters of synthetic membranes by hiperfiltration experiments, Part II: Membrane transport parameters independent of pressure and/or pressure difference. *Ber Bunsen Phys Chem*. 1977;81:854–864.

60. Abejón R, Garea A, Irabien A. Membrane process optimization for hydrogen peroxide ultrapurification. *Comput Aided Chem Eng*. 2011;29:678–682.
61. Fariñas M. *Osmosis inversa: fundamentos, tecnología y aplicaciones*. Madrid: McGraw-Hill, 1999.
62. Medina San Juan JA. *Desalación de aguas salobres y de mar: osmosis inversa*. Madrid: Mundi-Prensa, 2000.
63. Yang L, Eng Gan C. Costing small cleanrooms. *Build Environ*. 2007;42:743–751.
64. Rumsey Engineers, Inc. *Energy efficiency baselines for cleanrooms*. Non-Residential New Construction and Retrofit Incentive Programs of PG&E, Oakland, 2009.
65. Shaalan HF, Sorour MH, Tewfik SR. Simulation and optimization of a membrane system for chromium recovery from tanning wastes. *Desalination*. 2000;141:315–324.
66. Goosen MFA, Sablani SS, Al-Hinai H, Al-Obeidani S, Al-Belushi R, Jackson D. Fouling of reverse osmosis and ultrafiltration membranes: a critical review. *Sep Sci Technol*. 2004;39:2261–2297.
67. Avlonitis SA, Kouroumbas K, Vlachakis N. Energy consumption and membrane replacement cost for seawater RO desalination plants. *Desalination*. 2003;157:151–158.

Manuscript received Oct. 31, 2011, and revision received Jan. 19, 2012.